Bioinspiration & Biomimetics

TOPICAL REVIEW

Organismal aggregations exhibit fluidic behaviors: a review

IOP Publishing Bioinspir. Biomim. 14 (2019) 031001 https://doi.org/10.1088/1748-3190/ab0253

Bioinspiration & Biomimetics

TOPICAL REVIEW

Organismal aggregations exhibit fluidic behaviors: a review

Nicholas M Smith[1], Andrew K Dickerson[1,3] and David Murphy[2]

[1] Department of Mechanical and Aerospace Engineering, University of Central Florida Orlando, Florida, United States of America
[2] Department of Mechanical Engineering, University of South Florida Tampa, Florida, United States of America
[3] Author to whom any correspondence should be addressed.

E-mail: dickerson@ucf.edu

RECEIVED
2 October 2018

REVISED
7 January 2019

ACCEPTED FOR PUBLICATION
28 January 2019

PUBLISHED
26 February 2019

Keywords: density, phase change, viscosity, surface tension, swarming, flocking, schooling

Abstract

Groups of organisms such as flocks, swarms, herds, and schools form for a variety of motivations linked to survival and proliferation. Their size, locomotive domain, population, and the environmental stimuli guiding motion make challenging the study of member interactions and global behaviors. In this review, we borrow principles and analogies from fluids to describe the characteristics of organismal aggregations, which may inspire new tools for the analysis of collective motion. Examples of fluid resemblance include open channel flow, droplet formation, and particle-laden flow. We show how the properties of density, viscosity, and surface tension have strong parallels in the structure and behavior of aggregations of contrasting scale and domain. In certain cases, aggregations are sufficiently fluid-like that values can be assigned to such properties. We highlight how organisms engaging in collective motion can flow, roll, and change phase. Finally, we present limitations and exceptions for the application of fluidic principles to the motion of living groups.

1. Introduction

Organisms form groups, or aggregations, for myriad benefits including enhanced foraging, protection from predators, increased locomotive efficiency and migration, and access to mates [1–10]. However, group membership may also come at the risk of being preyed on by conspecifics [11, 12] and the local depletion of resources like oxygen [13]. Groups are thus presumed to form when the collective benefit of group membership outweighs the cost to individual organisms [5]. These groups may be comprised of a single species or may incorporate multiple species [14–16]. Such aggregations can number from just a few individuals to billions and do so across kingdoms, from large mammals to birds, insects, fish, and bacteria. These groups are classified as swarms, flocks, schools, herds, and packs according to animal type, group form, and function [5, 17–20]. Swarming, for example, is traditionally a term assigned to the collective behavior of groups of flying insects and sometimes to disorganized groups of swimming organisms and is not extended to terrestrial agents. To resolve this limitation in terminology, we use the term 'aggregation' to specify any grouping of similar organisms engaging in collective behavior.

The collective motion of organismal aggregations such as bird flocks and fish schools with hundreds or thousands of members has long intrigued observers. The extraordinary coordination of such aggregations seems to be enabled by high-frequency interactions among group members as each member individually responds to signals, such as changes in position or acceleration, provided by other group-mates [21]. However, the study of aggregation form and movement is often complicated by the large number of individuals comprising the group. Ideally, one can know the spatial position of each member with time, but as populations grow into the hundreds and beyond, size and occlusion can make the task nearly impossible [22]. The best techniques available use multiple cameras from various angles, known as stereophotogrammetry [23], and have been applied to airborne bird flocks and insect swarms and to aquatic fish and krill schools. If the spatial and temporal positions of all members is known, or at least well-approximated, one can extract aggregate density, polarity, packing fraction, nearest neighbor distance, and nearest neighbor position. Due to these challenges, many studies [22, 24–27] have departed from direct measurements and have attempted to characterize collective motions with mathematical models. One of the simplest of these is the Boids program [28].

From a broad Eulerian perspective, organismal aggregations resemble collections of like particles that interact with one another, share mutual attraction and repulsion, and flow in their respective environments. The diversity amongst organisms participating in collective behavior is nearly as varied as the methods and models used to study them, and science has yet to bring moderate unification to treatment of collective behavior. In this review, we present basic principles of fluid mechanics which may be used to interpret collective motion-phase, viscosity, and surface tension and highlight natural examples analogous to these principles. The organisms referenced herein, far from a comprehensive collection, span five orders of magnitude in size from midges to humans, eight orders of magnitude in number [22], and represent terrestrial, airborne, and aquatic domains.

2. Phase

2.1. Density and compressibility

Density is defined as the degree of compactness of a substance and has physical units of mass per volume. For fluids, large density is achieved by heavy and closely-packed molecules, and liquids are thus denser than gases. In the context of organismal aggregations, density may be characterized in a number of ways, to examine how inter-member spacing elicits particular aggregate behaviors. In general, the grouping of conspecifics to a threshold density enables information transfer and collective behavior through interactions between members [5, 29]. The simplest metric of aggregation density ρ is the number of individuals N in a given area A (in two dimensions) or volume V (in three dimensions), without regard to the mass of the individual. However, definition of the boundary of the aggregation area or volume is not straightforward [30]. The presence of inclusions within the aggregation or concave regions on the border mean that simple approaches such as a convex hull poorly represent the true aggregation area or volume [31]. Instead, it is first necessary to determine the minimum scale of concavities which characterize the aggregation and then to account for those using an alpha-shape algorithm which identifies concavities larger than this minimum scale and excludes them from the area or volume [31]. An alternative metric of density in organismal aggregations is the packing fraction, which takes into account both the aggregation density and the organism area or volume. The need for this metric is motivated by observing that the packing of an aggregation of 100 starlings in a cubic meter is much greater than the packing of 100 bees in that same volume [30]. In three-dimensional aggregations, the volume occupied by an organism often is represented by a sphere with radius r, and the packing fraction is thus $\phi = 4/3\pi\rho r^3$, which is the ratio between the volume individually occupied by the collection of N spheres and the aggregation volume as a whole. However, it should be noted that some elongated organisms such as fish and bacteria are better represented by ellipsoids than by spheres [32], and the corresponding ellipsoidal packing fraction would then be $\phi_e = 4/3\pi\rho abc$, where a, b, and c are the ellipsoid's principal semi-axes. Gases are dilute and thus have a low packing fraction whereas the packing fraction of liquids is substantially greater.

Organism aggregation density is a frequently collected metric of aggregation structure and varies greatly based on animal size, aggregation packing, and external conditions such as light level and the threat of predators [33]. For example, minnows may have school densities [34–36] of approximately 5000 members m^{-3}, and Murphy *et al* [63] measured Antarctic krill (*Euphausia superba*) schools with densities of 2492–18 860 m^{-3}. In contrast, migrating European starling flocks (*Sturnus vulgaris*), which may have in excess of 2000 members [31], have internal densities from 0.04–0.8 m^{-3}. Airborne swarms of locusts may have densities [37] of 0.001–0.05 m^{-3}. Densities and packing fractions are thus generally much higher in water than air. An explanation of this difference awaits a thorough comparison of aerial and aquatic aggregations across species. The maximum packing fraction of flocking starlings (figures 1(a) and (b)) has been measured as $\phi = 0.012$, which is comparable to a gas phase [31]. In contrast, the packing fraction of schooling Antarctic krill (figures 1(c) and (d)), assuming that an ellipsoid with $a = 53$ mm, $b = 10$ mm, and $c = 16$ mm matches the body shape of this animal, is $\phi = 0.15$. Similarly, the packing fraction of schools of golden shiners has been measured [38] as slightly less than $\phi = 0.25$. These values place krill and fish schooling closer to the regime of a liquid phase.

A related and possibly more biologically relevant parameter related to aggregation density is the nearest neighbor distance. After all, each aggregation member does not have the capability to determine the aggregation density as a whole but instead can sense the distance from itself to a small number of neighbors [31] and adjust its own position accordingly. Nearest neighbor distances are often expressed in terms of a characteristic body dimension such as body length or wingspan. For starling flocks [31], Ballerini *et al* (2008) determined nearest neighbor distance distributions from three-dimensional reconstructions of two-dimensional images where individuals appear as particles as seen in figure 2(a), much like experimental use of particle image velocimetry (PIV). These researchers found that individual starlings retain a minimum average working distance from other members of 1–4 wingspans [31]. The reason for this spacing is unknown but the minimum density is likely bounded by communication limits and the maximum density bounded by high probability of collision with other members. Distributions of nearest neighbor distances in organismal aggregations are often well described by log-normal distributions [32, 39, 40].

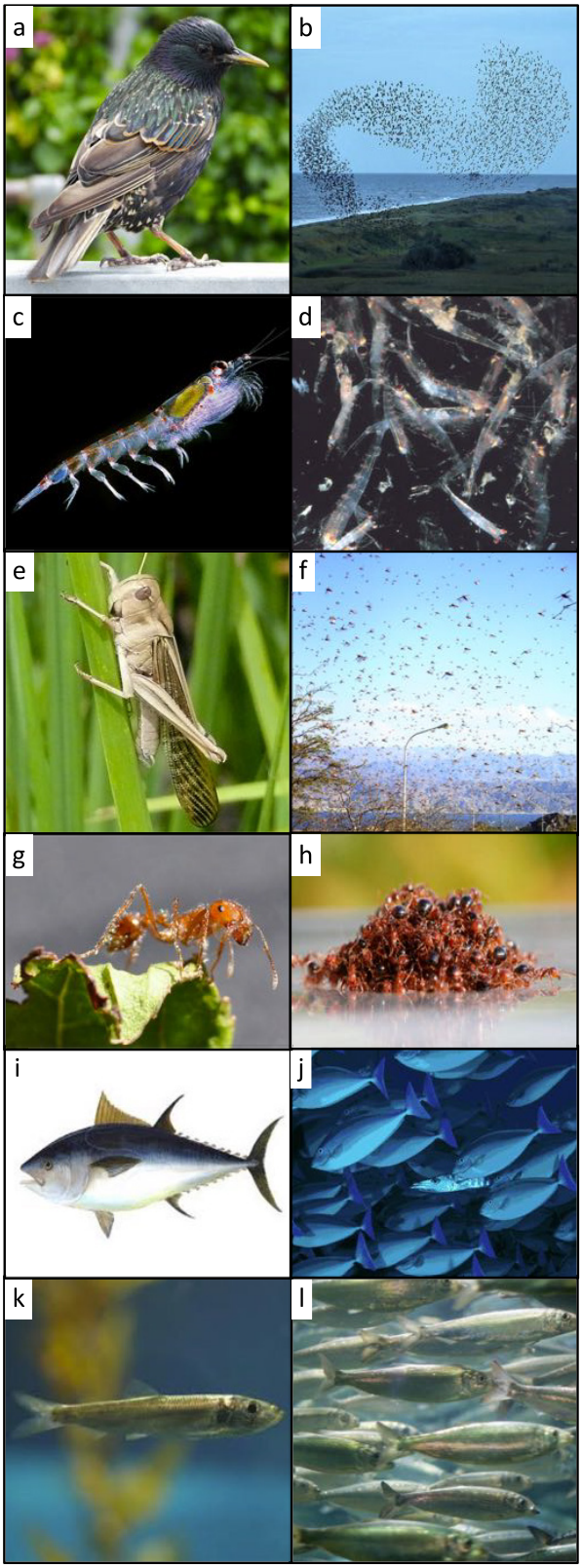

Figure 1. Images of (a) a starling [120] (CC BY-SA 2.0), (b) starling flock [121] (CC BY-SA 2.0), (c) Antarctic krill [122] (CC BY-SA 3.0), (d) swarming Antarctic krill [123] (https://commons.wikimedia.org/wiki/File:Krill swarm.jpg), (e) migratory locust [124] (CC BY-SA 3.0), (f) swarming locusts [125] (CC BY-SA 2.0), (g) fire ant [126] (CC BY-SA 2.0), (h) raft created by fire ants [43] (reproduced with author permission), (i) Atlantic tuna [127] (https://commons.wikimedia.org/wiki/File:Bluefin-big.jpg), (j) schooling tuna [128] (CC BY-SA 2.0), (k) herring [129] (CC BY-SA 2.5), (l) and schooling herring [130] (CC BY-SA 2.0). All images licensed for reuse unless otherwise specified.

A characteristic which both organismal aggregations and fluids share is that the density may not be homogeneous throughout the domain. For example, a compressible fluid droplet being acted upon by an external surface force would experience a pressure gradient in the fluid reflecting the higher density (or smaller distance between fluid molecules) in that region. A simple example of this phenomenon would

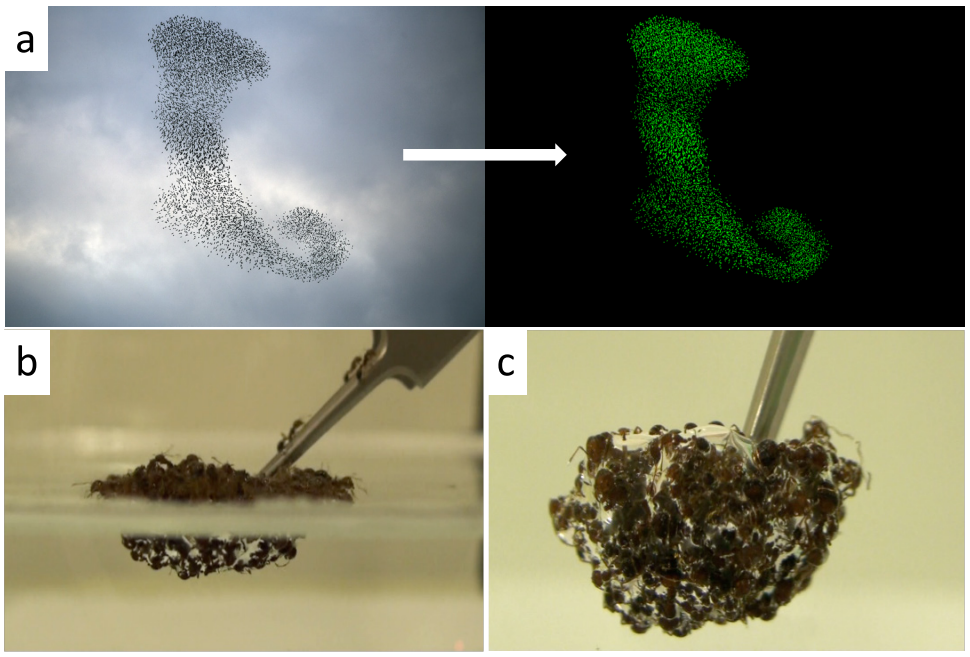

Figure 2. Images of (a) starling flock to be used for stereophotogrammetry (left) and the same image after post-processing where birds are treated as particles (right) [131] (CC BY 4.0). (b) Partially submerged fire ant raft [43], (c) fully submerged fire ant raft [43] (photo credits: Nathan Mlot & David Hu, Georgia Institute of Technology).

be the high-speed impact of an unyielding ball on an air-filled balloon. Similarly, organismal aggregations have heterogeneous density. Starling flocks, for example, exhibit variable density with anisotropic spacing throughout the flock volume [31]. Starling interactions rely on topological distance, meaning they rely on the motion of 6–7 of their neighbors to change direction and respond to perturbations, independent of their interstitial spacing [17, 26, 31, 41]. Heterogeneous density may be characterized in animal groups and in collections of particles by parameters such as the integrated conditional density and the pair distribution function [30].

As with unbounded fluids, starling flock volume is independent of the number of members [17, 31]. For example, a particular flock of $N = 530$ members amassed a cubic volume $V = 5470$ m^3, whereas a similar flock of $N = 1250$ had $V = 1840$ m^3. We plot V versus N data from Ballerini *et al* (2008) in figure 3. Such a spread in density does not allow for the calculation of a compressibility factor $Z = C \times (V/N)$, where C is an unknown constant, which we would expect to be nearly constant for conspecifics operating in comparable conditions [42]. However, variability in density may instead be akin to thermal expansion. Measurement of per member movement within a flock as a function of density is an area for future research.

Locusts, specifically *Locusta migratoria* (figures 1(e) and (f)) are known to amass swarms [22, 24] that dwarf starling flocks and can cover $>10^5$ acres. One study found the density of the airborne locust swarm is 0.001–0.5 m^{-3}, with roughly 2–4 m between neighboring flyers [37]. In contrast, a different study [1] documented localized density variations, with flying member separation as low as 0.1 m. Swarm density for populations in excess of a billion members is critical for cohesion. Minimal working distance would logically be driven by collision avoidance and maximum distance is capped when information transmission becomes imperceptible. Simulations of massive locust swarms show a pure attraction between members is not effective in modeling these swarms as the simulation tends to create tight spherical swarm models [27]. The addition of a repulsive term weighted greater than the attraction term for short length-scales results in a dispersed yet cohesive swarm model [24].

In contrast to flying aggregations, *Solenopsis invicta* ants (figure 1(g)) form cohesive clumps by grappling onto one another [43], seen in figure 1(h). The clumps of ants can spread, drip, and withstand applied loads, displaying elastic behavior [44]. A manifestation of this clump is the ant raft (figure 2(b)), which is formed by colonies during floods for survival [43, 45]. Ant rafts are porous, allowing them to be both strong and lightweight, and giving the raft buoyancy whilst prohibiting water ingress, as seen in figure 2(c). Paradoxically, ants cluster to greater densities (N/V) to form aggregate material densities (mass/V) that are lower than the individual ants' material density due to the ability of the clump to entrap air when fully or partially submerged. This behavior is analogous to a fluid immiscible with water and specific gravity less than unity floating atop a water surface. Unlike fluid molecules, ants do not move radially as the raft forms, but on average travel via random walks of 3.1 radii before settling on the raft edge [43].

2.2. Phase transition

Transitioning between phases is a common occurrence in many working fluids used today. A fluid may

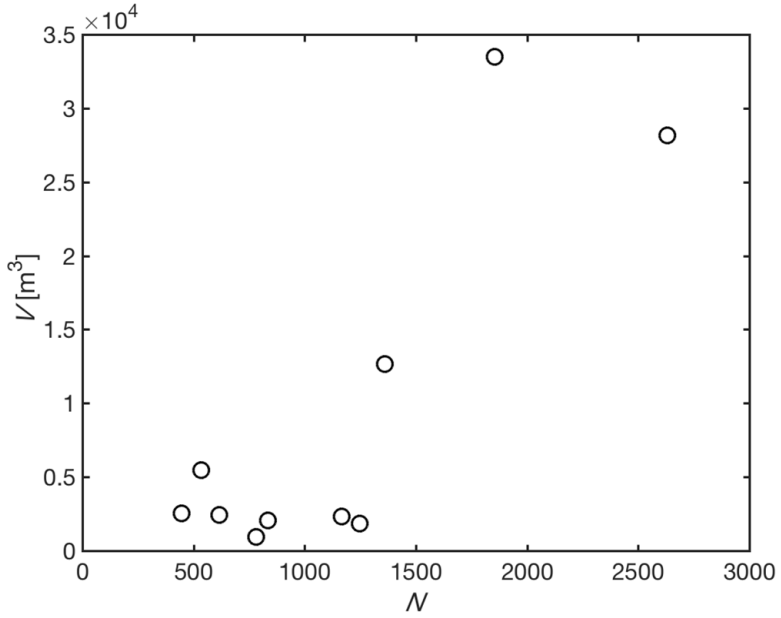

Figure 3. Starling flock volume as a function of flock population [31].

evaporate from a more organized phase (i.e. a liquid) to a less organized phase (i.e. a gas) through the addition of energy from heat or the reduction of pressure. Organismal aggregations also exhibit different levels of organization which can be characterized as different 'phases.' The transition between phases occurs in a manner analogous to evaporation and condensation, which is accompanied by changes in temperature and pressure. Temperature is a measure of the thermal motion of molecules, and pressure a measure of the physical molecular interactions in bounded fluids. The organismal analog to temperature is the increased physical activity of individuals, which increases the likelihood of physical interactions between members (pressure) so long as there is no commensurate increase in aggregate volume.

The phase of both fluids and organismal aggregations is related to the level of organization. A convenient means to characterize organismal organization is polarity. The polarity P of an aggregation is the mean of the deviation of each organism from the mean direction of the aggregation. Values of P range from $P = 90°$ for a completely disorganized group to $P = 0°$ for a perfectly aligned group [46]. The polarization order parameter O_P is another such metric of organization or phase and is calculated as the absolute value of the average of the heading vectors of all organisms within the aggregation [38]. Values of O_P range from $O_P = 1$ for a group in which all individuals are perfectly aligned to $O_P = 0$ for a group of individuals with random alignments. For example, Murphy *et al* [63] found mean values of $P = 34°$ and $O_P = 0.78$ for a group of Antarctic krill strongly schooling over an eight minute time period, values which indicate a high level of organization. Similarly, polarity values [47, 48] of 39°–63° and polarization order parameter values of 0.63–0.84 have been measured for small schools of fish [49]. Cavagna *et al* (2010) measured polarization in the range of $O_P = 0.844$–0.995 for flocking starlings, indicating extremely high levels of organization and coordination among group members. At the other end of the spectrum, swarms of midges exhibit little tendency to align with conspecifics and have polarization values of $O_P < 0.09$ [8]. For fluids, gaseous flows would be expected to be less organized (with longer travel distances for individual molecules) and thus exhibit higher P and lower O_P than liquid flows. Further, polarity and polarization order also can be estimated for common fluid flows. Laminar pipe flow, in which all fluid particles move in the same direction, would produce $P = 0°$ and $O_P = 1$, whereas turbulent pipe flow would produce a P slightly greater than zero and O_P slightly less than one. In contrast, stationary homogeneous isotropic turbulence would be expected to produce $P = 90°$ and $O_P = 0$. These parameters thus can convey organizational and directional information about both fluid flow and the motion of organism aggregations.

Transition from one phase to another may be triggered by the need to forage or mate or in response to external threats. However, the process by which this transition occurs is not well understood. Animal aggregations provide many examples of phase transitions which are analogous to those found in fluids. For example, the formation and dissolution of locust swarms is analogous to vapor condensing into liquid and evaporating back to vapor. Though several studies have examined locusts in their natural environment [50–52], field experiments with locust swarms are difficult because of the immense size of their aggregations. For example, a single *Locusta migratoria* swarm may spread across 100 km^2, exceed 10^{10} members, and its center of mass may travel up to 100 km a day [22, 24, 27]. Thus an understanding of locust swarm

formation has begun to emerge from experiments performed in laboratory settings with the insects tethered or enclosed in a small arena. Swarming develops as individuals cluster ($O(10)$ members), growing to form terrestrial 'marching bands' that collect additional members as they travel [24, 53]. Locust movement in bands is accompanied by an increase in O_P as solitary locusts congregate and display net migration. Locust nymphs, juvenile and flightless, utilize cannibalization when forming marching bands to establish and maintain collective movement [1, 11]. When members get too close, they bite one another, which in turn promotes motion. Adult marching bands take to the air at a critical mass which is subject to wind, temperature, and sunlight, a complex relationship which is not well-understood [24, 54, 55]. The process of locust aggregation and transition to flight is comparable to the formation of raindrops, as low O_P vapor molecules nucleate onto water-insoluble particles in the atmosphere [56] during phase change. At a critical size, the droplet falls and continues to collect vapor molecules during its travel. Yet another analogy is the flocculation and subsequent settling of suspended bacteria [57].

Schistocerca gregaria locusts likewise provide an analogue of phase transitions in fluids. These insects have two phases, a gregarious (liquid) and solitary (vapor) phase, each of which is associated with changes in behavior [18, 54]. To illustrate the resemblance to fluidic phase transition, we employ a generic temperature-specific volume (T-v) diagram in figure 5. A rise in in temperature and pressure corresponds to increases in internal energy, and increases in specific volume denote reduction in locust aggregate density. The cyclic nature of swarm formation and disbandment begins at (i), a saturated vapor, the point where solitary locusts are poised to assemble. Accompanying such a phase change is a decrease in internal energy, i.e. depleted levels of stored food energy. In a vapor, a drop in energy reduces molecular motion, resulting in a phase transition, with accompanying organization and cohesion (liquid). Forced crowding, which raises insects' serotonin levels, occurs as the insects transition from phase (i) to (ii). Serotonin is produced as a result of tactile, visual, and olfactory detection of other locusts. Within approximately 2 h of forced crowding [18, 27] the serotonin levels increase sufficiently to elicit full transition to the gregarious phase, state (ii). Foraging commences at (ii) and continues to (iii) as the cohesive swarm [22] rolls through thousands of acres increasing internal energy (stored food energy), temperature, and pressure, until the locusts are satiated at (iii). Next, the swarm dissolves as members leave the group and transition back to a solitary state, from (iii) to (iv). From (iv) to (i), the locusts expend energy to the point where internal energy drops sufficiently to drive the cycle again.

Another example of a phase transition in organismal aggregations is the transition from swarming to schooling exhibited by Antarctic krill. In the context of Antarctic krill behavior, a school is defined as an organized aggregation in which the group members are highly aligned (much like a fish school), and a swarm is an aggregation in which the group members are not well aligned (figures 4(a) and (b)). Antarctic krill are considered obligate schoolers and are extremely social [58]. Schools of Antarctic krill have been observed to travel for up to 12 km per day and sustain this pace for several days [59]. Upon finding food, the krill school breaks up into a swarm as animals individually feed [60]. The transition from schooling to swarming and back to schooling is difficult to study in the field, has not been well characterized, and is not well understood. However, recent laboratory studies in large schooling aquaria at the Australian Antarctic Division have begun to shed some light on Antarctic krill schooling [61–63]. For example, Murphy *et al* [63] used an overhead stereophotogrammetry system to examine how krill position themselves relative to their nearest neighbors and relative to the propulsion jet that each animal produces. School density, polarity, swimming speed, and nearest neighbor distance distributions also were characterized. Using the same system on a different day, Kanagawa *et al* (2012) captured and analyzed one instance of an unorganized Antarctic krill swarm transitioning into a well-organized school swimming around the periphery of a 1.432 m diameter cylindrical tank [64]. This phase transition (described below) took place over 45 min, and group statistics were characterized at 3 min intervals.

The aggregation polarity and mean swimming speed of the Antarctic krill as a function of time is shown in figure 4(c). Over the first 10 min, the aggregation is initially disordered with $P = 74$–$80°$, and mean krill swimming speed was approximately 35 mm s^{-1}. In the 10–20 min time period, the polarity dipped slightly, and the speed increased slightly. The polarity substantially decreased around the 30 min mark and, except for a spike at the subsequent time point, remained at a decreased value of approximately 35°. This spike likely represents a time point at which a gap in the schooling krill left a small number of disorganized animals in the field of view. High variability in the number of imaged krill and thus in the polarity was possible because the stereophotogrammetric field of view in this experiment covered only about 6 percent of the aquarium's surface area. The speed of individuals gradually increased throughout this transition to a maximum value of 60 mm s^{-1} at the experiment conclusion. Interestingly, as shown by figure 4(d), the Antarctic krill maintained a mean nearest neighbor distance (NND) of approximately one body length (40 mm) throughout the entire swarming-to-schooling transition, especially since increased density has been thought to trigger school formation [39]. It is also interesting to note that, in contrast to the rapid transition (on the order of seconds) between phases observed in fish schools [38], the transition for Antarctic krill takes several minutes. Data capturing such transitions is difficult to acquire but lends great insight into the dynamics of phase

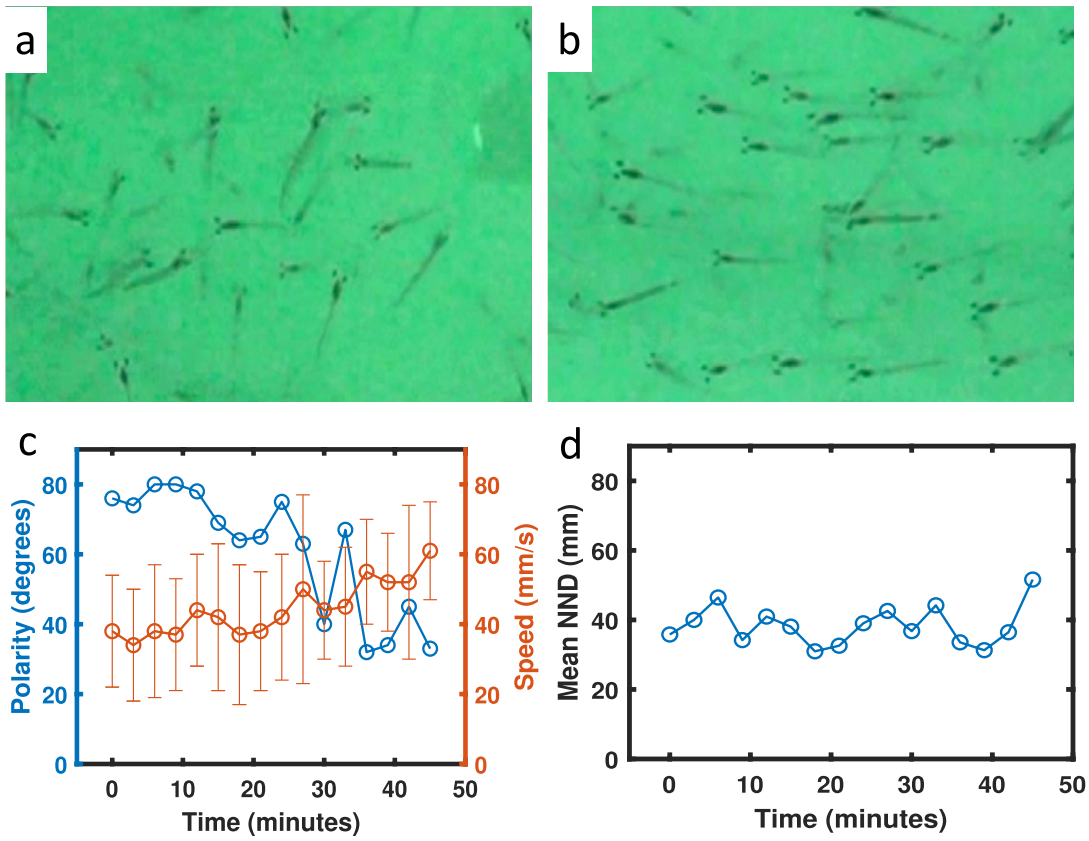

Figure 4. (a) Sample image of swarming Antarctic krill with high polarity, (b) sample image of schooling Antarctic krill with low polarity, (c) time series of Antarctic krill aggregation polarity and mean krill swimming speed as the aggregation transitions from unorganized swarming to organized schooling. Error bars indicate standard deviation. (d) Corresponding time series of mean nearest neighbor distance (NND).

transition and the time scales across which they may occur. However, a greater understanding of the interactions and information transfer among conspecifics facilitating such transitions is needed to fully characterize this phenomenon.

Changes in phase also may be tied to changes in the behavior of organisms within an aggregation. For example, crowd density heavily influences individual human behavior [65]. A crowd of pedestrians can treated as a continuum so long as the typical distance between members is much less than the characteristic length scale of the space in which they are moving [65, 66]. At sufficient velocities, humans exhibit flow separation around flow obstacles [66]. Crowds are approximately locally homogeneous, forming body-centric square patterns with high degrees of polarity [67]. In the 1990s, studies of crowd motion abandoned the use of Navier–Stokes equations and derived equations which merge unsteady continuity and social theories, including functions for walking speed and discomfort as a function of density [65, 66]. These nonlinear partial differential equations are amenable to an analytic solution and are applicable to unsteady flows. Furthermore, they result in two flow regimes, subcritical (tranquil) and supercritical (rapid) flow, defined by wave-like motion that can appear in the flow, similar to highway patterns [68]. Thus, crowds maintain a strong parallel to open channel flow [69, 70]. At very high crowd densities, the equations of motion resemble two-dimensional Navier–Stokes equations with Newtonian friction replaced by Rayleigh-like friction, and generally neglect advective terms.

2.3. Multiphase flow

Multiphase flow, in which both a continuous fluid phase and dispersed phase (e.g. gas or vapor bubbles, immiscible liquid droplets, or solid particles) are important, may serve as a useful model for heterospecific organismal aggregations. Though most animal groups comprise a single species, some animals including birds [71], ungulates [72, 73], fish [74], primates [75], and cetaceans [76] form heterospecific aggregations. Benefits of heterospecific aggregations are thought to include enhanced detection of food and predators [75]. For example, giraffes have good eyesight, an elevated vantage point from which to scan for predators, and high vigilance. Zebras forming a herd with giraffes, as seen in figure 6(a), are thus able to eavesdrop on the cues provided by the giraffes, reduce their own vigilance, and feed more effectively [73]. Multiphase flow also may serve as a useful model for conspecifics of different sizes within an aggregation. Fish and Antarctic krill, for example, may form schools comprising animals of different sizes [77, 78], and herds of ungulates often contain both adults and juveniles with different locomotive

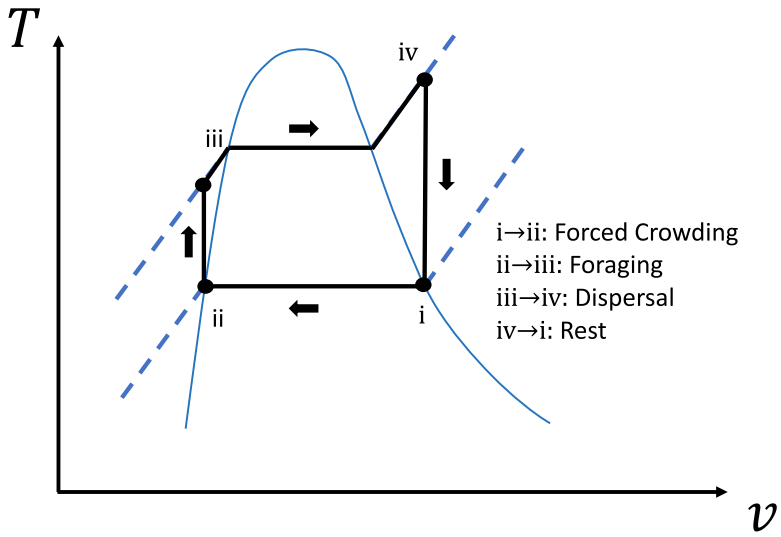

Figure 5. Temperature (T) versus specific volume (v) diagram relating locust phase change to phase change in a typical two-phase working fluid.

and sensory capabilities. However, both schooling mackerel and herring (figures 1(k) and (l)) have been found to remain in close proximity with similarly sized neighboring conspecifics, a preference which may relate to the increased hydrodynamic efficiency of schooling [79].

In a modeling framework comparing heterospecific aggregations with multiphase flows, the heterospecifics (or conspecifics of different sizes) can be thought of as particles with different physical characteristics such as size, mass, shape, and drag dispersed in a continuous fluid phase. These physical characteristics may then be used to model dynamical aspects of group behavior in response to an external stimulus. Stimuli may include actual physical influences such as gravity, wind, and turbulence, or analogous physical influences (sociobiological pressures) such as predation. For example, in a simple thought experiment, a cloud of initially well-mixed crude oil droplets with a bimodal size distribution with diameter peaks at 0.4 mm and 0.1 mm diameter suspended in seawater could be compared to a school of krill containing both adults and juveniles. Such clouds have a wide range of droplet sizes and occur when an oil well blowout creates a turbulent jet of oil and gas on the sea floor. The resulting plume rises to the free surface due to droplet buoyancy [80–82]. The 0.4 mm diameter oil droplets have a substantially greater rise speed at 10 mm s^{-1} than 0.1 mm droplets at 0.8 mm s^{-1}, just as adult krill swimming is several times faster than juvenile krill [83]. Thus, a population of initially well-mixed droplets with a bimodal size distribution will completely separate into two distinct populations after some time [84]. This phenomenon is illustrated for a wide distribution of oil droplet sizes rising in artificial seawater in figure 6(b) [80]. In figure 6(a), we present an oil cloud created by a jet moving from right to left. The the youngest portion of the oil cloud, on the lefthand side, is the most well-mixed, containing droplets of various size. In contrast, the oil cloud is well fractionated on the righthand side, with millimeter-scale droplets exiting the top of the field of view and micron-scale droplets below. A similar phenomenon has been reported in swimming Antarctic krill schools with different size classes, as seen in figure 6(c) [77]. As observed by scientific divers, an initially well-mixed swimming school with large and small krill eventually elongated and pinched into two separate schools. The leading school contained large, faster swimming animals while the other contained smaller krill with slower swimming speeds. Similarly, a herd of peccaries fleeing a predator will leave behind more slowly running juveniles [85]. In these examples, fear of predation provides the 'force' for krill school and peccary herd division and is analogous to the buoyant force fractionating droplet clouds. As a final example, granular flow of differently sized or shaped particles through a pipe could provide an analogy to the motion of a mixed-species or mixed-age herd of sheep or cattle within a chute [86].

The fluid dynamics of interactions among clouds of dispersed bubbles, droplets, or solid particles also bears similarities to hydrodynamic interactions in organismal aggregations such as fish schools. For example, in the draft-kiss-tumble sequence undergone by two inline, interacting, sedimenting spheres, the trailing sphere sinks at a higher speed than a single sphere sinking alone due to the wake of the leading sphere [87]. Similarly, some swimming animals such as jellyfish and krill [62] drag a parcel of fluid behind them through the viscosity-enhanced mechanism of Darwin's drift [88], and occupying this 'drafting' position has been suggested as a method of saving energy for schooling animals [63]. In addition, the transport of a dispersed particle phase by an external flow, such as blowing dust or snow, is a classic multiphase flow phenomenon paralleled by organis-

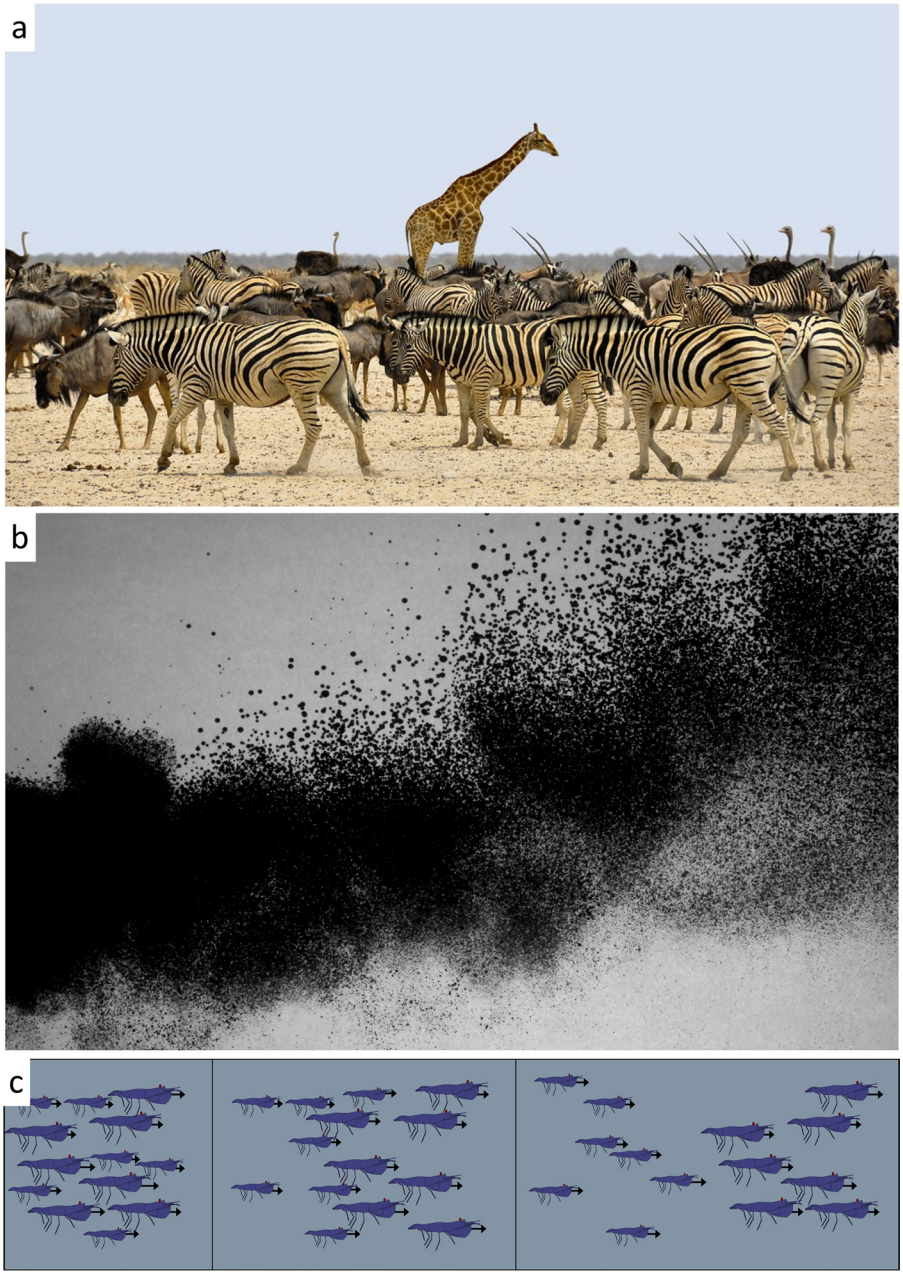

Figure 6. Examples of (a) multi-species aggregations with zebras and giraffe [132], (b) a plume of crude oil droplets with a micron-to-mm size distribution fractionating by size as droplets rise in water at different speeds [80] (John Wiley & Sons. © 2016. American Geophysical Union. All Rights Reserved), and (c) depiction of fractionation by differences in swimming speed in a krill school with a bimodal size distribution.

mal aggregations taking advantage of environmental flows, such as swarming locusts riding the wind [27]. Locusts seeding the wind is made possible by their low density and high drag profile [89, 90]. In comparable flow visualization experiments, seed particles are chosen to have a sufficiently low Stokes number by which to follow streamlines. Taking off against the wind, the locusts turn with the wind once airborne and fly forward until they reach front-most edge of the group [24, 27, 37]. Once at the front they land and forage until the overhead swarm has passed them and then re-initiate flight remaining in the swarm.

3. Viscosity

Viscosity is the resistance of a fluid to deformation in response to an externally applied shear stress. A fluid's viscosity allows neighboring fluid particles to influence one another through this shear stress. Here, we highlight how members of aggregations 'shear' one another, through physical contact, or social pressures and interactions between neighbors. Near-neighbor interactions give aggregations form and responsiveness, and allow boundary conditions to impact the behavior of the entire group. Clumps

of *Solenopsis invicta* ants provide such an example. Researchers measured the continuum property of viscosity of ant clusters by considering ants as molecules and subjecting the clusters to rheometry tests. The viscosity of ant groups was measured as $\sim 10^6$ cP by allowing a sphere to settle into a beaker of ants, as a sphere might sink into a viscous fluid [44], with a corresponding shear rate of $\dot{\gamma} = 1.9 \times 10^{-3}$ s^{-1}. In a plate-plate rheometer, the stress required to maintain the imposed ant flow was approximately constant at 70 Pa for $\dot{\gamma} = 10^{-3}$ s^{-1} to 10^{1} s^{-1}. Thus, the ant aggregations shear thin dramatically with increasing shear rate. Experiments with live and dead ants produce identical values of viscosity, indicating that ants become passive when forced to flow. Live ants subjected to a constant stress creep and maintain constant strain rates. A ball of ants, for example, placed on water surface slumps to form a flattened raft, much like when a drop of viscous fluid spreads on a solid surface [43], behaving as a porous material [43, 91, 92] with density of ≈ 0.2 g ml^{-1}. Under oscillatory strain, ant aggregations are viscoelastic, able to store and dissipate energy, similar to colloidal gels of Brownian particles in a solvent [44]. The possibility of viscoelastic behavior in aggregations of animals which flow in response to external perturbations but are unable to link together does not seem to have been explored.

In organismal aggregations which do not physically link with each other, such as flocks of birds and schools of fish, viscosity may be analogous to social forces. For example, humans in crowds do not enjoy being in contact with one another. As crowd density increases, motion slows as if the crowd's viscosity increases, strengthening the friction as individuals slide past one another [93]. Rates of passage though halls and doors drop dramatically if this viscous nature is not controlled [94]. A particularly high profile example is the fatal 2015 Mina stampede that occurred on the Jamaraat Bridge in Saudi Arabia, a result of critically high crowd congestion [95]. This disaster followed a similar incident [96] and bridge redesign in 2004. Surprisingly, placing a barrier in a flow of pedestrians at a building exit can decrease the travel time of all those exiting by preventing jamming at the door threshold and increase flow rate through the exit [94]. This phenomenon, known as Braess' paradox, can perhaps be extended to preventing clogs of particle-laden flows with high Bagnold numbers [97], $\mathrm{Ba} = \rho_p d^2 \lambda^{1/2} \dot{\gamma} / \mu$, where ρ_d is the particle density, d is the particle diameter, λ is the linear particle concentration, and μ is the interstitial fluid viscosity. Such an extension to particle-laden flow jamming has not been explored in the literature to the authors' knowledge. Herds of sheep and cattle also likely experience a type of viscosity as they flow through a gate into a pen or along a fence. This viscosity seems to be a result of closely packed (e.g. congested) neighbors interfering with their neighbors' ability to locomote freely.

4. Surface tension

Surface tension refers to the propensity of liquids to behave elastically at a liquid–air interface and arises from intermolecular attraction. A liquid is more attracted to itself than the surrounding gas. Surface tension enables droplet cohesion and the ability to reform shape after perturbation. The same can be said for organismal aggregations such as schools, flocks, and clumps of ants that have coherent boundaries and maintain structure throughout aggregate motion. Individuals within these groups are similarly more attracted to their neighbors than to the surrounding void. This attraction may comprise physical links or a social force between conspecifics. These groups thus have the ability to self-heal and reform in response to environmental perturbations and threats. The aggregative social dynamics which cohere animal groups through a surface tension-like force have long been used to model the collective movement of animal groups. The Boids model, for example, successfully recreated realistic flocking behavior by requiring members steer to avoid crowding nearby conspecifics, steer so as to align with nearby conspecific, and steer towards the center of mass of the aggregation [98]. This last rule is a useful analogue of surface tension as it provides an inward pull towards the group center.

Ants are well known for their ability to collectively accomplish tasks ranging from foraging to tunneling to construction [43–45, 99, 100]. The method by which ants build bridges [101] and floating rafts [43], by grappling onto nearest neighbors [99], is particularly pertinent to this review as it illustrates how organismal aggregations can resist external forces and maintain shape. While individual ants do not behave like fluid molecules and while the interactions between ants grappling onto one another are quite different from molecular interactions, the contiguous mass created by this behavior exhibits surface tension-like properties. Grappling ant groups will, for example, drip from a downward hanging point like water droplets dripping or flow from a leaky faucet [91, 92], like that seen in figure 7(a). When shaken about in a beaker, ants readily grapple together and form a ball which may be stretched and pulled apart by hand [43]. The strength of the 'ant-fluid' material is a function of the number of grappling connections ants make with neighbors and the length of those linkages [99], as seen in figures 7(b) and (c). On average, an ant connects at 6 points to its neighbors and is connected to 4.8 different neighbors. If a ball of ants is briefly compressed between two plates, they will spring back to nearly its original shape once the external force is removed

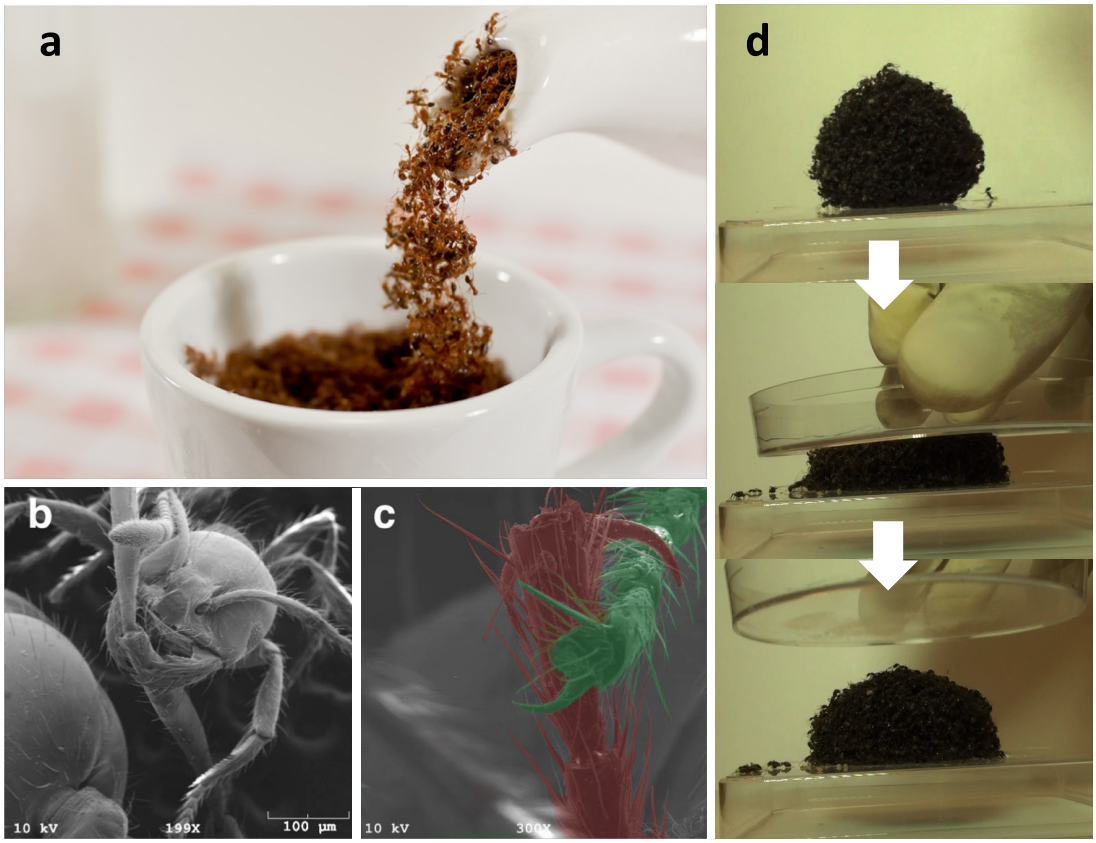

Figure 7. (a) Ants pouring from a teapot, and SEM images of ant-to-ant linkages (b) with mandible-tarsus [43], and (c) tarsus-tarsus linking [43], and (d) a cluster of ants being compressed between two parallel plates and regaining form when compression is released. Photo credits: Nathan Mlot & David Hu, Georgia Institute of Technology.

[44], as seen in figure 7(d). This repeatable behavior corresponds to how a water droplet behaves when compressed between two superhydrophobic surfaces. Researchers estimated the surface tension of a cluster, $\sigma = F/\delta \sim 10^3$ dyn cm^{-1} by measuring ant grappling force F and spacing δ, and found a value that is 10 times the surface tension of water for a raft that is one-fifth the density of water [43]. The resulting capillary length for ants is 3 cm. A fluid with such properties would have a droplet spreading time of 10^3 seconds, nearly an order of magnitude greater than the spreading time of an ant raft. The tendency of some prey fish species, such as herring (figures 1(k) and (l)) to form into cohesive balls [102], large spherical aggregations on which dolphins, orcas [103, 104], and seabirds feed, also reveals an aggregative social force analogous to the surface tension which pulls a small water droplet into a spherical shape [105].

Stationary midge swarms of *Dasyhelea flavifrons*, *Corynoneura scutellata*, and *Cladotanytarsus atridorsum* provide surface tension-like behavior, but are in stark contrast to ants, as members do not grapple one another. Instead, social forces provide the attraction needed to keep a cohesive aggregation. Midge swarms are comprised primarily of males and seek to attract females for reproduction [4, 106, 107]. The swarms have a zero mean velocity [8] and assemble at landmarks [108]. They take the shape of columns, as pictured [109] in figure 8(a), which are generally 2 m above ground, range from 1–5 m in height, and are comprised of approximately 10^2–10^4 members [110]. It has been shown that midges influence each other's motion far beyond their nearest neighbors [4]. Member attraction to the center of the swarm enables cohesion [4, 8], and is a result of non-polar alignment with one another. This non-polarizing behavior is comparable to freely moving particles which rebound at the surface to reorient for ballistic flight toward the center [8]. Flight tracks of individual midges are shown [9] in figure 8(b). Within the swarm, midges fly in a zig–zag pattern both horizontally and vertically [111] and experience 3–4 g when changing direction at the swarm surface, where acceleration is highest [8, 112]. Acceleration is zero as midges pass through the center. Maximum speed in laboratory conditions was found [112] to be around 1.1 m s^{-1}, corresponding to a Reynolds number range of Re = 240–280.

5. Discussion

One of the challenges with studying aggregate behavior is natural variation and structure from one group to another. In our review, we found large discrepancies in group sizes and spacing. Locust swarm spacing was reported by one study [1] as low as 0.1 m between flyers, another [37] reported 2–4 m,

Figure 8. (a) Midges congregating to form columns of midge swarms for reproductive purposes [109] and (b) tracking of midges detailing 3D trajectories inside the swarm [9]. Copyright (2014) by the American Physical Society.

and yet another [54] reported 1 individual per 10 m. An analog in fluids would be the comparison between standard-pressure and rarefied gases [113]. The large size of flocks, swarms, and schools likewise present challenges in their characterization. Across literature there is great variety in experimental methodology and data presentation for aggregations, even within the same type and species. Starling densities have been reported by nearest neighbor distance and members per volume [31, 41], while others report density only qualitatively [114]. Variety in methods and values produces a lack of consistency that may be addressed by employing some of the analogies described in this review.

Care must be taken, however, when using fluid principles to describe groups of animals. There are numerous behaviors and characteristics within all locomotive domains which cannot be resolved by considering groups of conspecifics as fluid in form. Perhaps the simplest example is the no-slip boundary condition. A crowd moving through a passageway does not establish the flow profile predicted by Couette flow, but more closely resembles that of inviscid plug flow. Namely, people against walls do not have zero velocity. This observation may be explained by calculation of a Knudsen number $\mathrm{Kn} = \ell/L$ for human crowds [115], where ℓ is the mean free path and L is some representative physical length scale, perhaps the width of a hallway or footpath. Henderson (1974) concluded human crowd motion must be treated as free particle flow, not continuum flow [115]. Perhaps in some scenarios, those against a wall can travel most quickly because of fewer potential collisions with neighbors. By extension, viscous boundary layers can be absent or inverse. Other studies likewise conclude that at very low human crowd densities, treating human movement as a continuum becomes ineffective and it is better to consider discrete pedestrians [65, 116, 117]. Human groups also have the ability to walk though each other in differing directions by using interstitial space to avoid contact, which has no analogue in continuum flows [65], but can be described by applying the kinetic theory of rarefied gasses [118], which has been done sparsely in the literature. Ants in a rheometer likewise do not obey no-slip [44]. To obtain ant assemblage viscosity, researchers used Velcro on rheometer plates to entangle ant tarsi and thereby artificially create a no-slip condition.

The Reynolds number is perhaps the most ubiquitous and beloved dimensionless group in fluid mechanics, but the reader may notice there is no mention of its use above to describe the behavior of a group, only individuals. The assignment of a Reynolds number to individuals in flight or swimming is straightforward so long as an appropriate length scale is known, but assigning appropriate values of density, length, and viscosity for moving groups is unclear. Presume we want to apply a Reynolds number to compare bird flocks and we know average flock density (mass/volume), a length scale given by flock volume and exterior surface area, and flock mean speed. Assignment of a viscosity is not straightforward, and it is likely that viscous effects are heavily tied to packing fraction, and thus density. The assignment of a Reynolds number, and other common dimensionless groups in fluid mechanics, is an area for further consideration. Additionally, what would a Reynolds number for a flock, school, herd, or swarm convey about the group? A comparably high Reynolds number would indicate a group has comparably high inertia, but at present does not provide insight to characteristics of motion. For example, will a high Reynolds number aggregation transition to turbulent and chaotic motion? Densely packed *Bacillus subtilis* bacteria can self-sustain tur-

bulence at low Reynolds numbers, which shares qualitative characteristics with classical small-scale turbulence because the bacteria act as a living fluid [119]. It is unlikely there is a parallel within macroscale organisms, and such a notion is currently absent from literature and an area for future work.

Acknowledgments

We would like to thank the University of Central Florida and the University of South Florida for funding this work. Certain images in this publication have been obtained by the author(s) from the Wikipedia/Wikimedia website, where they were made available under a Creative Commons licence or stated to be in the public domain. Please see individual figure captions in this publication for details. To the extent that the law allows, IOP Publishing disclaim any liability that any person may suffer as a result of accessing, using or forwarding the image(s). Any reuse rights should be checked and permission should be sought if necessary from Wikipedia/Wikimedia and/or the copyright owner (as appropriate) before using or forwarding the image(s).

ORCID iDs

Nicholas M Smith https://orcid.org/0000-0003-2507-0358
Andrew K Dickerson https://orcid.org/0000-0003-1220-1048
David Murphy https://orcid.org/0000-0002-9852-4085

References

[1] Ariel G and Ayali A 2015 Locust collective motion and its modeling *PLoS Comput. Biol.* **11** e1004522
[2] Alerstam T, Hedenström A and Åkesson S 2003 Long-distance migration: evolution and determinants *Oikos* **103** 247–60
[3] Hemelrijk C K and Hildenbrandt H 2012 Schools of fish and flocks of birds: their shape and internal structure by self-organization *Interface Focus* **2** rsfs20120025
[4] Attanasi A *et al* 2014 Collective behaviour without collective order in wild swarms of midges *PLoS Comput. Biol.* **10** e1003697
[5] Vicsek T and Zafeiris A 2012 Collective motion *Phys. Rep.* **517** 71–140
[6] Sarà G, Dean J, d'Amato D, Buscaino G, Oliveri A, Genovese S, Ferro S, Buffa G, Martire M L and Mazzola S 2007 Effect of boat noise on the behaviour of bluefin tuna thunnus thynnus in the mediterranean sea *Mar. Ecol. Prog. Ser.* **331** 243–53
[7] Partridge B L 1982 The structure and function of fish schools *Sci. Am.* **246** 114–23
[8] Kelley D H and Ouellette N T 2013 Emergent dynamics of laboratory insect swarms *Sci. Rep.* **3** 1073
[9] Chaté H and Muñoz M A 2014 Insect swarms go critical *Physics* **7** 120
[10] Ni R and Ouellette N T 2016 On the tensile strength of insect swarms *Phys. Biol.* **13** 045002
[11] Bazazi S, Buhl J, Hale J J, Anstey M L, Sword G A, Simpson S J and Couzin I D 2008 Collective motion and cannibalism in locust migratory bands *Curr. Biol.* **18** 735–9
[12] Simpson S J, Sword G A, Lorch P D and Couzin I D 2006 Cannibal crickets on a forced march for protein and salt *Proc. Natl Acad. Sci.* **103** 4152–6
[13] Brierley A S and Cox M J 2010 Shapes of krill swarms and fish schools emerge as aggregation members avoid predators and access oxygen *Curr. Biol.* **20** 1758–62
[14] Mills K L 1998 Multispecies seabird feeding flocks in the galápagos islands *Condor* **100** 277–85
[15] Korneliussen R J, Heggelund Y, Eliassen I K and Johansen G O 2009 Acoustic species identification of schooling fish *ICES J. Mar. Sci.* **66** 1111–8
[16] Hulet C, Anderson D, Smith J, Shupe W, Taylor C Jr and Murray L 1989 Bonding of goats to sheep and cattle for protection from predators *Appl. Animal Behav. Sci.* **22** 261–7
[17] Hildenbrandt H, Carere C and Hemelrijk C K 2010 Self-organized aerial displays of thousands of starlings: a model *Behav. Ecol.* **21** 1349–59
[18] Anstey M L, Rogers S M, Ott S R, Burrows M and Simpson S J 2009 Serotonin mediates behavioral gregarization underlying swarm formation in desert locusts *Science* **323** 627–30
[19] Newlands N K, Lutcavage M E and Pitcher T J 2006 Atlantic bluefin tuna in the gulf of maine, I: estimation of seasonal abundance accounting for movement, school and school-aggregation behaviour *Environ. Biol. Fishes* **77** 177–95
[20] White K, Lewis M and Murray J 1996 A model for wolf-pack territory formation and maintenance *J. Theor. Biol.* **178** 29–43
[21] Herbert-Read J E 2016 Understanding how animal groups achieve coordinated movement *J. Exp. Biol.* **219** 2971–83
[22] Topaz C M and Bertozzi A L 2004 Swarming patterns in a two-dimensional kinematic model for biological groups *SIAM J. Appl. Math.* **65** 152–74
[23] Hedrick T L 2008 Software techniques for two-and three-dimensional kinematic measurements of biological and biomimetic systems *Bioinspiration Biomimetics* **3** 034001
[24] Topaz C M, Bernoff A J, Logan S and Toolson W 2008 A model for rolling swarms of locusts *Eur. Phys. J. Spec. Top.* **157** 93–109
[25] Stöcker S 1999 Models for tuna school formation *Math. Biosci.* **156** 167–90
[26] Hereford J M and Blum C 2011 Flockopt: a new swarm optimization algorithm based on collective behavior of starling birds *NaBIC* pp 17–22
[27] Edelstein-Keshet L 2001 Mathematical models of swarming and social aggregation *Proc. of the 2001 Int. Symp. on Nonlinear Theory and its Applications (Miyagi, Japan)* (Pennsylvania, PA: Citeseer) pp 1–7
[28] Phelan S E 1999 A note on the correspondence between complexity and systems theory *Systemic Pract. Act. Res.* **12** 237–46
[29] Karaboga D 2005 An idea based on honey bee swarm for numerical optimization *Technical Report* Technical report-tr06, Erciyes University, Engineering Faculty, Computer Engineering Department
[30] Cavagna A, Cimarelli A, Giardina I, Orlandi A, Parisi G, Procaccini A, Santagati R and Stefanini F 2008 New statistical tools for analyzing the structure of animal groups *Math. Biosci.* **214** 32–7
[31] Ballerini M *et al* 2008 Empirical investigation of starling flocks: a benchmark study in collective animal behaviour *Animal Behav.* **76** 201–15
[32] Olsen D and Murphy D 2018 Random sequential addition simulations of animal aggregations (submitted)
[33] O'brien D 1989 Analysis of the internal arrangement of individuals within crustacean aggregations (euphausiacea, mysidacea) *J. Exp. Mar. Biol. Ecol.* **128** 1–30
[34] Pitcher T 1973 Some field measurements on minnow schools *Trans. Am. Fisheries Soc.* **102** 840–3
[35] Pitcher T 1973 The three-dimensional structure of schools in the minnow, phoxinus phoxinus (l.) *Animal Behav.* **21** 673–86
[36] Pitcher T and Partridge B 1979 Fish school density and volume *Mar. Biol.* **54** 383–94
[37] Edelstein-Keshet L, Watmough J and Grunbaum D 1998 Do travelling band solutions describe cohesive swarms? An investigation for migratory locusts *J. Math. Biol.* **36** 515–49

[38] Tunstrøm K, Katz Y, Ioannou C C, Huepe C, Lutz M J and Couzin I D 2013 Collective states, multistability and transitional behavior in schooling fish *PLoS Comput. Biol.* **9** e1002915
[39] Cambuí D S and Rosas A 2012 Density induced transition in a school of fish *Physica* A **391** 3908–14
[40] Becco C, Vandewalle N, Delcourt J and Poncin P 2006 Experimental evidences of a structural and dynamical transition in fish school *Physica* A **367** 487–93
[41] Ballerini M *et al* 2008 Interaction ruling animal collective behavior depends on topological rather than metric distance: evidence from a field study *Proc. Natl Acad. Sci.* **105** 1232–7
[42] Brodie J 1976 The flight behaviour of starlings at a winter roost *Br. Birds* **69** 51–60
[43] Mlot N J, Tovey C A and Hu D L 2011 Fire ants self-assemble into waterproof rafts to survive floods *Proc. Natl Acad. Sci.* **108** 7669–73
[44] Tennenbaum M, Liu Z, Hu D and Fernandez-Nieves A 2016 Mechanics of fire ant aggregations *Nat. Mater.* **15** 54
[45] Phonekeo S, Dave T, Kern M, Franklin S V and Hu D L 2016 Ant aggregations self-heal to compensate for the ringelmann effect *Soft Matter* **12** 4214–20
[46] Huth A and Wissel C 1992 The simulation of the movement of fish schools *J. Theor. Biol.* **156** 365–85
[47] Viscido S V, Parrish J K and Grünbaum D 2004 Individual behavior and emergent properties of fish schools: a comparison of observation and theory *Mar. Ecol. Prog. Ser.* **273** 239–49
[48] Tien J H, Levin S A and Rubenstein D I 2004 Dynamics of fish shoals: identifying key decision rules *Evolutionary Ecol. Res.* **6** 555–65
[49] Herbert-Read J E, Perna A, Mann R P, Schaerf T M, Sumpter D J and Ward A J 2011 Inferring the rules of interaction of shoaling fish *Proc. Natl Acad. Sci.* **108** 18726–31
[50] Baker P and Cooter R 1979 The natural flight of the migratory locust, locusta migratoria l *J. Comparative Physiol.* A **131** 79–87
[51] Rainey R C *et al* 1989 *Migration and meteorology. Flight behaviour and the atmospheric environment of locusts and other migrant pests* (Oxford: Oxford University Press)
[52] Waloff Z *et al* 1951 Field studies on factors affecting the displacements of desert locust swarms in Eastern Africa *Anti-Locust Bull* **9** 1–50
[53] Buhl J, Sumpter D J, Couzin I D, Hale J J, Despland E, Miller E R and Simpson S J 2006 From disorder to order in marching locusts *Science* **312** 1402–6
[54] Kennedy J S 1951 The migration of the desert locust (*schistocerca gregaria* Forsk.) I. The behaviour of swarms. II. A theory of long-range migrations *Phil. Trans. R. Soc.* B **235** 163–290
[55] Uvarov B *et al* 1977 *Grasshoppers and Locusts. A Handbook of General Acridology vol 2 Behaviour, Ecology, Biogeography, Population Dynamics* (London: Centre for Overseas Pest Research)
[56] Rosinski J and Kerrigan T 1969 The role of aerosol particles in the formation of raindrops and hailstones in severe thunderstorms *J. Atmos. Sci.* **26** 695–715
[57] Hassanpourfard M, Nikakhtari Z, Ghosh R, Das S, Thundat T, Liu Y and Kumar A 2015 Bacterial floc mediated rapid streamer formation in creeping flows *Sci. Rep.* **5** 13070
[58] Nicol S and Foster J 2003 Recent trends in the fishery for antarctic krill *Aquatic Living Resour.* **16** 42–5
[59] Kanda K, Takagi K and Seki Y 1982 Movement of the larger swarms of antarctic krill euphausia superba population off enderby land during 1976–1977 season *J. Tokyo Univ. Fisheries* **68** 24–42
[60] Hamner W M 1984 Aspects of schooling in euphausia superba *J. Crustacean Biol.* **4** 67–74
[61] Kawaguchi S, King R, Meijers R, Osborn J E, Swadling K M, Ritz D A and Nicol S 2010 An experimental aquarium for observing the schooling behaviour of antarctic krill (euphausia superba) *Deep-Sea Res.* II **57** 683–92
[62] Catton K B, Webster D R, Kawaguchi S and Yen J 2011 The hydrodynamic disturbances of two species of krill: implications for aggregation structure *J. Exp. Biol.* **214** 1845–56
[63] Murphy D *et al* 2018 The three dimensional spatial aggregation of antarctic krill schools *Sci. Rep.* **9** 381
[64] Kanagawa M, Murphy D, Webster D, Kawaguchi S, King R and Yen J 2012 Swarming to schooling transitions in antarctic krill aggregations *Integrative and Comparative Biology* vol 52 (Oxford: Oxford University Press)
[65] Hughes R L 2003 The flow of human crowds *Annu. Rev. Fluid Mech.* **35** 169–82
[66] Hughes R L 2002 A continuum theory for the flow of pedestrians *Transp. Res.* B **36** 507–35
[67] Smith R 1993 Volume flow rates of densely packed crowds *Engineering for Crowd Safety* (Amsterdam: Elsevier) pp 313–9
[68] Nomura Y, Saito S, Ishiwata R and Sugiyama Y 2016 Hopf bifurcation analysis for a dissipative system with asymmetric interaction: analytical explanation of a specific property of highway traffic *Phys. Rev.* E **93** 012215
[69] Gerhart P M, Gerhart A L and Hochstein J I 2016 *Munson's Fluid Mechanics* (New York: Wiley)
[70] Lighthill M J and Whitham G 1955 On kinematic waves I. Flood movement in long rivers *Proc. R. Soc.* A **229** 281–316
[71] Sasvári L 1992 Great tits benefit from feeding in mixed-species flocks: a field experiment *Animal Behav.* **43** 289–96
[72] Pays O, Ekori A and Fritz H 2014 On the advantages of mixed-species groups: impalas adjust their vigilance when associated with larger prey herbivores *Ethology* **120** 1207–16
[73] Schmitt M H, Stears K and Shrader A M 2016 Zebra reduce predation risk in mixed-species herds by eavesdropping on cues from giraffe *Behav. Ecol.* **27** 1073–7
[74] Ward A J, Axford S and Krause J 2002 Mixed-species shoaling in fish: the sensory mechanisms and costs of shoal choice *Behav. Ecol. Sociobiol.* **52** 182–7
[75] Stensland E, Angerbjörn A and Berggren P 2003 Mixed species groups in mammals *Mammal Rev.* **33** 205–23
[76] Frantzis A and Herzing D L 2002 Mixed-species associations of striped dolphins (*Stenella coeruleoalba*), short-beaked common dolphins (*Delphinus delphis*) and risso's dolphins (*Grampus griseus*) in the Gulf of Corinth (Greece, Mediterranean Sea) *Aquatic Mammals* **28** 188–97
[77] Hamner W M, Hamner P P, Strand S W and Gilmer R W 1983 Behavior of antarctic krill, euphausia superba: chemoreception, feeding, schooling and molting *Science* **220** 433–5
[78] Krause J and Godin J-G J 1994 Shoal choice in the banded killifish (*Fundulus diaphanus*, Teleostei, Cyprinodontidae): effects of predation risk, fish size, species composition and size of shoals *Ethology* **98** 128–36
[79] Pitcher T, Magurran A and Edwards J 1985 Schooling mackerel and herring choose neighbours of similar size *Mar. Biol.* **86** 319–22
[80] Murphy D W, Xue X, Sampath K and Katz J 2016 Crude oil jets in crossflow: effects of dispersant concentration on plume behavior *J. Geophys. Res.: Oceans* **121** 4264–81
[81] North E W, Adams E E, Thessen A E, Schlag Z, He R, Socolofsky S A, Masutani S M and Peckham S D 2015 The influence of droplet size and biodegradation on the transport of subsurface oil droplets during the deepwater horizon spill: a model sensitivity study *Environ. Res. Lett.* **10** 024016
[82] Zhao L, Boufadel M C, Socolofsky S A, Adams E, King T and Lee K 2014 Evolution of droplets in subsea oil and gas blowouts: development and validation of the numerical model vdrop-j *Mar. Pollut. Bull.* **83** 58–69
[83] Murphy D, Webster D, Kawaguchi S, King R and Yen J 2011 Metachronal swimming in antarctic krill: gait kinematics and system design *Mar. Biol.* **158** 2541
[84] Socolofsky S and Adams E 2002 Multi-phase plumes in uniform and stratified crossflow *J. Hydraul. Res.* **40** 661–72
[85] Byers J A and Bekoff M 1981 Social, spacing and cooperative behavior of the collared peccary, tayassu tajacu *J. Mammalogy* **62** 767–85
[86] Trulsson M 2018 Rheology and shear jamming of frictional ellipses *J. Fluid Mech.* **849** 718–40
[87] Fortes A F, Joseph D D and Lundgren T S 1987 Nonlinear mechanics of fluidization of beds of spherical particles *J. Fluid Mech.* **177** 467–83

[88] Katija K and Dabiri J O 2009 A viscosity-enhanced mechanism for biogenic ocean mixing *Nature* **460** 624
[89] Snelling E P, Becker C L and Seymour R S 2013 The effects of temperature and body mass on jump performance of the locust locusta migratoria *PLoS One* **8** e72471
[90] Kühsel S, Brückner A, Schmelzle S, Heethoff M and Blüthgen N 2017 Surface area–volume ratios in insects *Insect Sci.* **24** 829–41
[91] Bonabeau E, Theraulaz G, Deneubourg J-L, Lioni A, Libert F, Sauwens C and Passera L 1998 Dripping faucet with ants *Phys. Rev.* E **57** 5904
[92] Theraulaz G, Bonabeau E, Sauwens C, Deneubourg J-L, Lioni A, Libert F, Passera L and Solé R 2001 Model of droplet dynamics in the argentine ant linepithema humile (mayr) *Bull. Math. Biol.* **63** 1079–93
[93] Kirchner A, Nishinari K and Schadschneider A 2003 Friction effects and clogging in a cellular automaton model for pedestrian dynamics *Phys. Rev.* E **67** 056122
[94] Frank G A and Dorso C O 2011 Room evacuation in the presence of an obstacle *Physica* A **390** 2135–45
[95] Salamati P and Rahimi-Movaghar V 2016 Hajj stampede in Mina, 2015: need for intervention *Arch. Trauma Res.* **5** e36308
[96] Ahmed Q A, Arabi Y M and Memish Z A 2006 Health risks at the Hajj *Lancet* **367** 1008–15
[97] Bagnold R A 1954 Experiments on a gravity-free dispersion of large solid spheres in a newtonian fluid under shear *Proc. R. Soc.* A **225** 49–63
[98] Reynolds C W 1987 *Flocks, Herds and Schools: a Distributed Behavioral Model* (*ACM SIGGRAPH Computer Graphics* vol 21) (New York: ACM) pp 25–34
[99] Foster P C, Mlot N J, Lin A and Hu D L 2014 Fire ants actively control spacing and orientation within self-assemblages *J. Exp. Biol.* **217** 2089–100
[100] Hu D, Phonekeo S, Altshuler E and Brochard-Wyart F 2016 Entangled active matter: from cells to ants *Eur. Phys. J. Spec. Top.* **225** 629–49
[101] Reid C R, Lutz M J, Powell S, Kao A B, Couzin I D and Garnier S 2015 Army ants dynamically adjust living bridges in response to a cost–benefit trade-off *Proc. Natl Acad. Sci.* **112** 15113–8
[102] Nøttestad L and Axelsen B E 1999 Herring schooling manoeuvres in response to killer whale attacks *Can. J. Zool.* **77** 1540–6
[103] Pitman R L and Durban J W 2012 Cooperative hunting behavior, prey selectivity and prey handling by pack ice killer whales (orcinus orca), type b, in antarctic peninsula waters *Mar. Mammal Sci.* **28** 16–36
[104] Nøttestad L, Fernö A and Axelsen B E 2002 Digging in the deep: killer whales' advanced hunting tactic *Polar Biol.* **25** 939–41
[105] Clua É and Grosvalet F 2001 Mixed-species feeding aggregation of dolphins, large tunas and seabirds in the azores *Aquatic Living Resour.* **14** 11–8
[106] González M A *et al* 2017 Flight and swarming behaviour of culicoides species (diptera: Ceratopogonidae) on a livestock farm in northern spain *Veterinaria Ital.* **53** 157–66
[107] Blackwell A, Mordue A J, Young M R and Mordue W 1992 The swarming behaviour of the scottish biting midge, culicoides impunctatus (diptera: Ceratopogonidae) *Ecol. Entomology* **17** 319–25
[108] Downes J 1969 The swarming and mating flight of diptera *Annu. Rev. Entomology* **14** 271–98
[109] 2013 www.flickr.com/photos/ex_magician/9446381695
[110] Neems R M, Lazarus J and Mclachlan A J 1992 Swarming behavior in male chironomid midges: a cost-benefit analysis *Behav. Ecol.* **3** 285–90
[111] Okubo A and Chiang H 1974 An analysis of the kinematics of swarming ofanarete pritchardi kim (diptera: Cecidomyiidae) *Res. Population Ecol.* **16** 1–42
[112] McLachlan A, Ladle R and Crompton B 2003 Predator–prey interactions on the wing: aerobatics and body size among dance flies and midges *Animal Behav.* **66** 911–5
[113] Muntz E P 1989 Rarefied gas dynamics *Annu. Rev. Fluid Mech.* **21** 387–422
[114] Fernández-Juricic E, Siller S and Kacelnik A 2004 Flock density, social foraging and scanning: an experiment with starlings *Behav. Ecol.* **15** 371–9
[115] Henderson L F 1974 On the fluid mechanics of human crowd motion *Transp. Res.* **8** 509–15
[116] Helbing D, Keltsch J and Molnar P 1997 Modelling the evolution of human trail systems *Nature* **388** 47
[117] Hoogendoorn S and Bovy P 2000 Gas-kinetic modeling and simulation of pedestrian flows *Transp. Res. Rec.: J. Transp. Res. Board* **1710** 28–36
[118] Dogbe C 2012 On the modelling of crowd dynamics by generalized kinetic models *J. Math. Anal. Appl.* **387** 512–32
[119] Wensink H H, Dunkel J, Heidenreich S, Drescher K, Goldstein R E, Löwen H and Yeomans J M 2012 Meso-scale turbulence in living fluids *Proc. Natl Acad. Sci.* **109** 308
[120] 2012 www.flickr.com/photos/nottsexminer/7481510872
[121] 2017 https://commons.wikimedia.org/wiki/File:Starling_Murmuration_-_RSPB_Minsmere_(21446738793).jpg
[122] 2012 https://commons.wikimedia.org/wiki/File:Antarctic_krill_(Euphausia_superba).jpg
[123] 2005 https://commons.wikimedia.org/wiki/File:Krill_swarm.jpg
[124] 2009 https://commons.wikimedia.org/wiki/File:Locusta_migratoria_migratorioides_male.jpg
[125] 2004 www.flickr.com/photos/antichrist/34263448
[126] 2014 www.flickr.com/photos/rick_hagerty/14268239017
[127] 2012 https://commons.wikimedia.org/wiki/File:Bluefin-big.jpg
[128] 2007 www.flickr.com/photos/davidview/1197037450
[129] 2018 https://commons.wikimedia.org/wiki/File:Clupea_pallasii_by_OpenCage.jpg
[130] 2007 www.flickr.com/photos/jakecaptive/885981258
[131] 2014 www.smithsonianmag.com/smart-news/scientists-use-twitter-pics-study-spiders-ants-and-birds-180970237/
[132] 2016 https://pixabay.com/en/zebra-gnu-giraffe-africa-namibia-1170177/